SSCL-389

SSCL-389

Superconducting Super Collider Laboratory

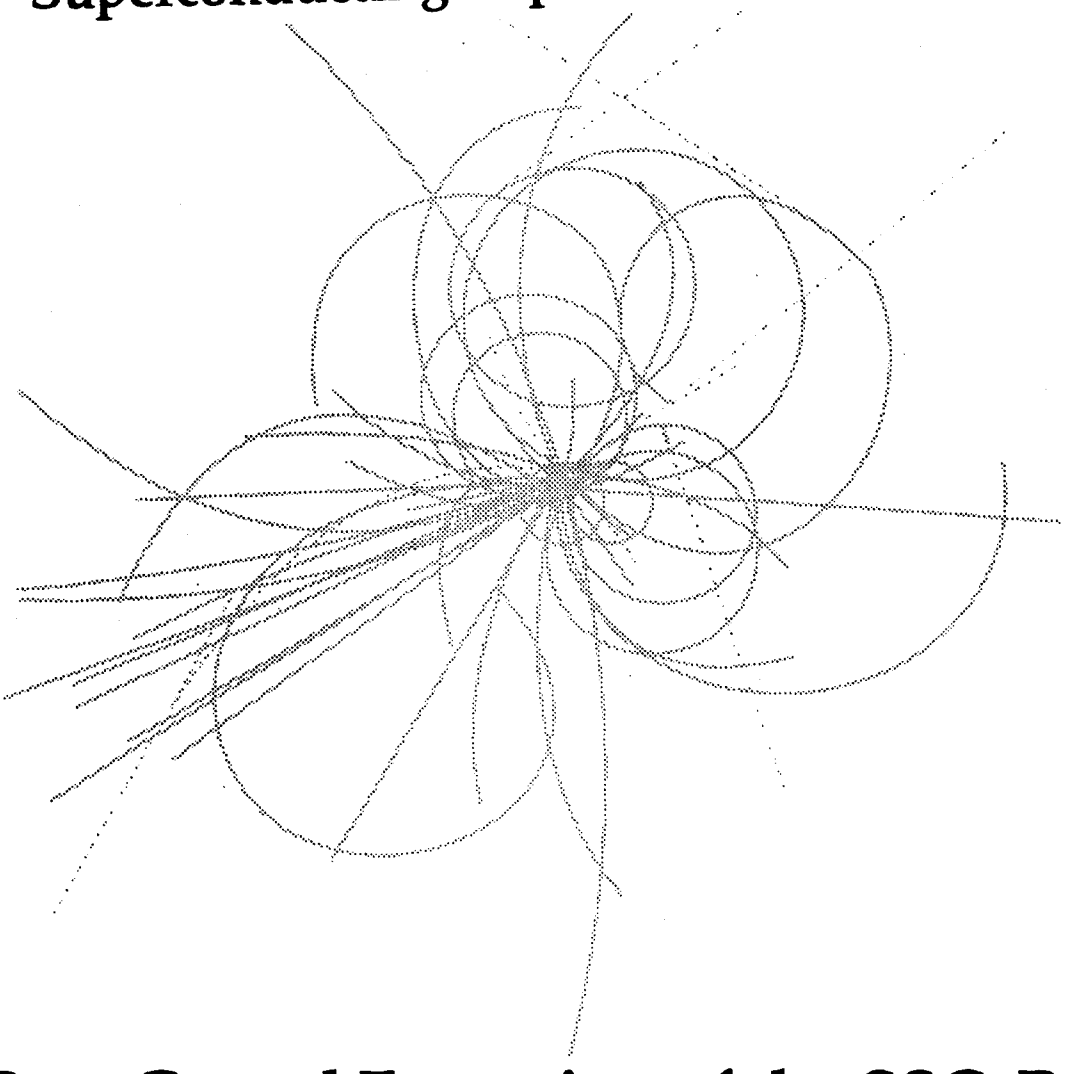

# Bent Crystal Extraction of the SSC Beam with RF Noise Induced Diffusion

H.-J. Shih and A. Taratin

March 1991

SSCL-389

# Bent Crystal Extraction of the SSC Beam with RF Noise Induced Diffusion

H.-J. Shih

Superconducting Super Collider Laboratory*
2550 Beckleymeade Avenue
Dallas, TX 75237

and

A. M. Taratin

Nuclear Physics Institute
634050 Tomsk USSR

March 1991

* Operated by the Universities Research Association, Inc., for the U.S. Department of Energy under Contract No. DE-AC02-89ER40486.

SSCL-389

# Bent Crystal Extraction of the SSC Beam with RF Noise Induced Diffusion

H.-J. Shih and A. M. Taratin


## Abstract

Channeling of charged particles in bent crystals has been considered for use in parasitic extraction of the Superconducting Super Collider (SSC) beam. To make this feasible, a small fraction of the SSC proton beam must be brought onto a bent crystal. In this paper, the method of introducing filtered phase noise into the rf system to diffuse the tails of the beam was investigated using computer simulations. The channeling efficiency of an incident beam by a bent silicon crystal was then analyzed using a theory and simulations. In addition, the increase in channeling efficiency because of the possibility of multiple passage through the crystal was studied in the presence of the injected filtered rf noise.

## 1.0 INTRODUCTION

There are advantages to conducting B physics experiments in a fixed-target configuration at the Superconducting Super Collider (SSC) rather than in a collider configuration.[1,2] In order not to interfere with collider operations, the extracted beam should have an intensity of $\sim 10^8$ protons per second, which would produce $\sim 10^{10}$ $B\overline{B}$ pairs per year. The interest generated by this prospect resulted in a proposal for a Super Fixed Target Beauty Facility (SFT) at the SSC.[2] Presently, the best procedure for extracting a 20 TeV beam from the SSC appears to be through the use of proton channeling in a bent crystal inserted in the beam tail.[1–4] It was originally thought that the forward-peaked, quasi-elastic scattered halo from IRs and beam-gas scattering could be used as the source of the extracted beam. However, it was shown that this source was insufficient to sustain an extraction rate of $10^8$ protons per second.[5] The idea of producing a large amplitude beam halo by (1) injecting a small amount of noise into the rf system and (2) generating some dispersion in the lattice at the position of the crystal was then studied.[6] This was shown to be feasible using a turn-to-turn uncorrelated phase noise. In Section 2, the simulation results from investigating this extraction technique using filtered noise will be presented.

It is envisioned that the extraction will be done in the East utility straight section, where a horizontal dogleg will be inserted (see Figure 1). A schematic picture of the SSC with the extraction elements is shown in Figure 2. A bent Si crystal, placed approximately 200 m upstream of the Lambertson string, intercepts a portion of the circulating proton beam and deflects it vertically so that it is separated from the circulating beam by 2 cm in the Lambertson string and passes the field free region. The required bending angle, $\theta_B$, is then

$$\theta_B = \frac{2\,\mathrm{cm}}{200\,\mathrm{m}} = 100\,\mu\mathrm{rad}.$$

The limit of bending while maintaining channeling is determined by the critical bend radius[7,8] $R_c$, which is 33.3 m for a Si crystal and an incident energy of 20 TeV. To avoid serious bending dechanneling, experiments[9] suggest that the bending radius $R$ should be one order of magnitude greater than the limiting radius $R_c$ in order to obtain substantial transmission. This suggests a crystal length $S$:

$$S = 10 \times 33\,\mathrm{m} \times 100\,\mu\mathrm{rad} \simeq 3\,\mathrm{cm}.$$

To trap significant numbers of particles in the channeling regime, the vertical beam divergence $\sigma_{y'}$ has to be smaller than the channeling critical angle[10,11] $\theta_c$, which is approximately 1 $\mu$rad for the (110) planes of Si at 20 TeV. Since the vertical beta function is always greater

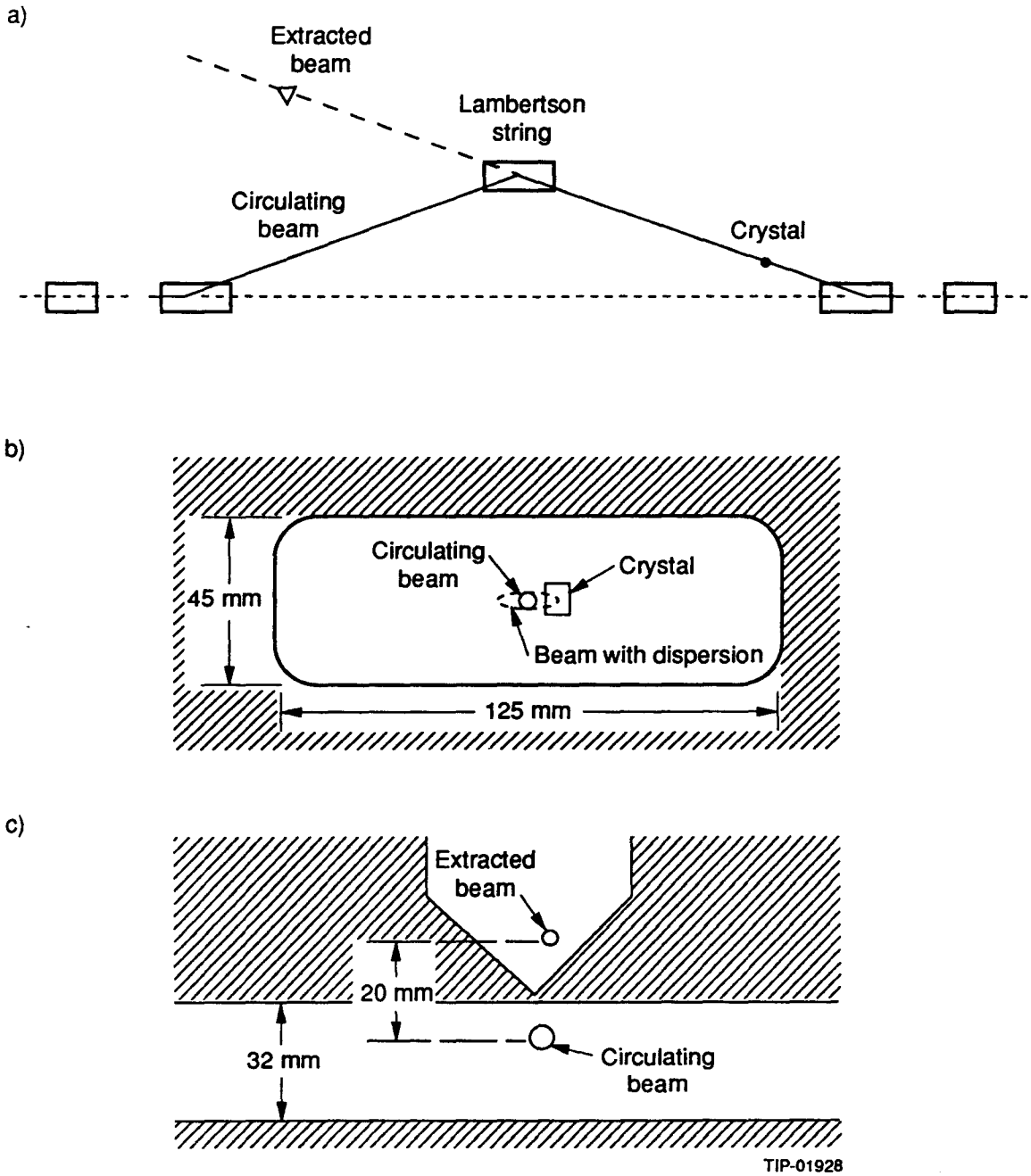


Figure 1. Proposed Extraction Scheme. (a) The horizontal doglet with a bent crystal inserted about 200 m upstream of the Lambertson string. The dashed line with an arrow indicates the extracted beam line. (b) The cross-sectional view at the position of the crystal. Using large dispersion in combination with rf noise induced diffusion, a small fraction of the beam intercepts the crystal. (c) The cross-sectional view in the Lambertson string. The extracted beam, which is the portion of the beam that the bent crystal intercepts and deflects vertically, has been separated from the circulating beam by 2 cm and passes the field-free region.

than 500 m in the drift space of the East utility straight and the SSC normalized emittance is 1 mm·mrad, we have

$$\sigma_{y'} \lesssim 0.3\,\mu\text{rad}.$$

Assuming a Gaussian distribution, the angular acceptance is then 99% or more. Particles incident on a crystal may also fail to be channeled if they strike within the fraction of the cross-sectional area of the crystal face occupied by the atoms making up the crystal planes. This is the so-called surface acceptance effect, and it accounts for as much as a 20% loss for Si (110) planes. A particle initially trapped in the channeling regime may become dechanneled in the crystal due to electron multiple scattering and the lattice vibrations. This effect is measured by the dechanneling half-length $S_{1/2}$, which is the length over which one-half of initially channeled particles are lost by the dechanneling process. At 20 TeV, $S_{1/2} \simeq 12\,\text{m}$ for Si. Thus the multiple scattering dechanneling is negligible for a Si crystal of length 3 cm. The capture efficiency, i.e., the probability that a particle which strikes a Si crystal bent along (110) planes is initially trapped in the channeling regime, and the dechanneling half-length will be determined quantitatively in Section 3 using a theory and simulations.

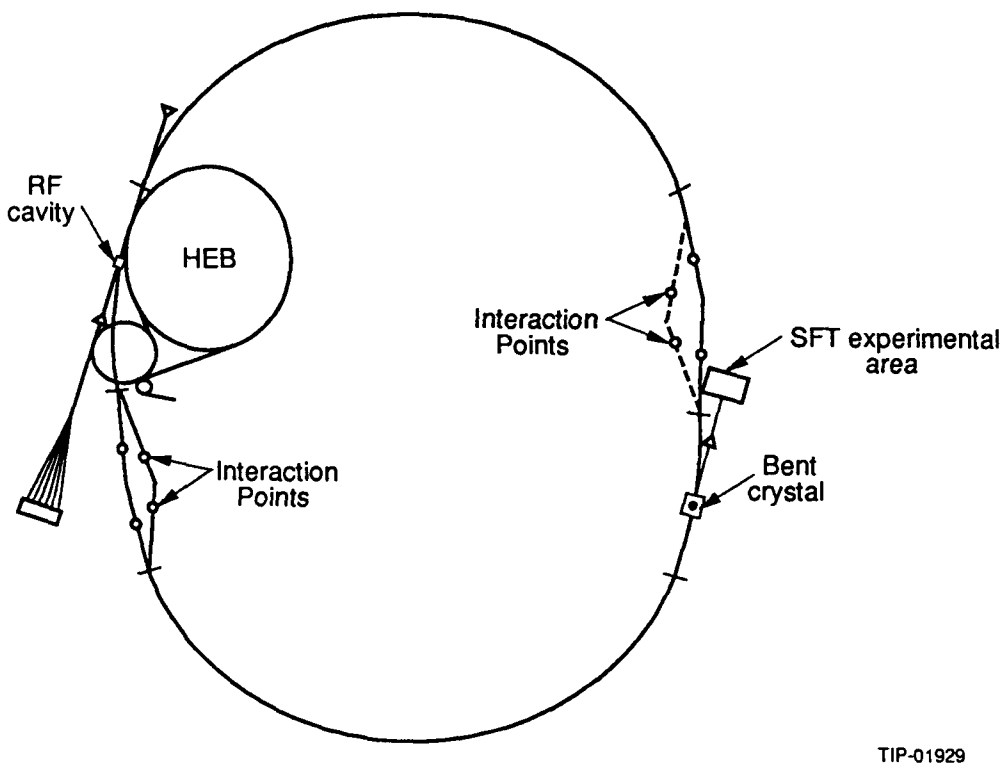


Figure 2. Layout of the SSC with the Extraction Elements: RF System in the West Utility Straight, Bent Crystal in the East Utility Straight, External Beam Line for Extraction and SFT Experimental Area.

The protons which enter the crystal but are not channeled and those dechanneled traverse the crystal as an amorphous material. A small fraction of these are lost due to nuclear inelastic collisions (about 3% or more for a Si crystal of length 3 cm). However, because the extraction line is in the storage ring, those that survive can be channeled on subsequent passes. The increase in channeling efficiency due to multiple passage will be evaluated using simulations in Section 4. Conclusions will be given in Section 5.

## 2.0 DIFFUSING PARTICLES USING FILTERED RF NOISE

Some protons in the circulating beam have to be brought onto the bent crystal for extraction. One way to achieve this is to introduce a small amount of noise into the rf system. This has been demonstrated in a previous study[6] using turn-to-turn uncorrelated phase noise. This noise affects the whole beam, and in fact it was found that particles which hit the crystal came rather uniformly from the whole beam. It was then suggested that filtered noise might be able to affect the core less but the tails more. In this section, our computer simulations using filtered phase noise are described and the results presented. We found that in the filtered case, the particles which hit the crystal came from the tails, not the core.

Particle tracking was conducted in a linear lattice for the SSC. Two transfer matrices are used to transport the particles from the bent crystal to the rf cavity and back to the crystal. To each particle six independent variables are assigned: horizontal coordinate $x$, horizontal angle $x'$, vertical coordinate $y$, vertical angle $y'$, path length deviation from the ideal trajectory $l$, and fractional momentum deviation from the ideal momentum $\delta$. The construction of the transfer matrices applied to the vectors $(x, x', y, y', l, \delta)$ can be found in the Appendix of Reference 6. The rf cavity (bent crystal) is placed at the north end of the quadrupole QU4 (QU1) north (south) of the utility straight center in the West (East) campus. Table 1 lists the values of the alpha $(\alpha_x, \alpha_y)$, beta $(\beta_x, \beta_y)$, and dispersion functions $(\eta)$ at these two locations, along with the tune shifts $Q_x, Q_y$ and distance $\Delta s$ from one location to the other. The parameters at the position of the crystal were from a recent modification to the lattice to provide a high dispersion region in the East utility straight.[12] The other relevant parameters are: normalized emittance $\epsilon_N = 1\,\text{mm·mrad}$, collider circumference $C_0 = 87120\,\text{m}$, momentum compaction factor $\alpha_c = 9.6 \times 10^{-5}$, harmonic number $h = 104544$, and peak rf voltage $V = 20\,\text{MV}$.

One thousand particles are launched at the bent crystal. The initial values of $x, x', y, y', l$, and $\delta$ are randomly generated according to Gaussian distributions. We assume the initial energy standard deviation from 20 TeV to be 1 GeV, i.e., $\sigma_\delta = 0.5 \times 10^{-4}$. The

Table 1. Some Relevant Accelerator Parameters.

| parameter | @ bent crystal | @ rf cavity |
|---|---|---|
| $\alpha_x$ | 0.28 | 0.11 |
| $\alpha_y$ | $-0.68$ | 3. |
| $\beta_x$ | 359.88 m | 44.68 m |
| $\beta_y$ | 516.87 m | 440.2 m |
| $\eta$ | $-4.$ m | 0. m |
| $\eta'$ | 0. | 0. |
| $Q_x$ | $61.24^a$ | $62.05^b$ |
| $Q_y$ | $61.55^a$ | $61.72^b$ |
| $\Delta s$ | $43338.6^a$ m | $43781.4^b$ m |

[a]From the bent crystal to the rf cavity.
[b]From the rf cavity to the bent crystal.

initial standard deviations $x, x', y, y'$, and $l$ are determined from the following relationships:

$$\sigma_{x,y} = \sqrt{\frac{\epsilon_N \tilde{\beta}_{x,y}}{\gamma}},$$

$$\sigma_{x',y'} = \sqrt{\frac{\epsilon_N}{\gamma \tilde{\beta}_{x,y}}},$$

$$\sigma_l = \left(\frac{C_0 \alpha_c}{T_0 \Omega}\right) \sigma_\delta ,$$

where $\tilde{\beta}$ is the beta function in the principal frame, $\gamma$ is the ratio of the particle's total energy to its rest energy, $T_0$ is the revolution period, and $\Omega$ the small amplitude synchrotron frequency. Using the alpha and beta functions at the position of the bent crystal, we obtain the following initial standard deviations: $\sigma_x = 0.13\,\mathrm{mm}$, $\sigma_{x'} = 0.36\,\mu\mathrm{rad}$, $\sigma_y = 0.16\,\mathrm{mm}$, $\sigma_{y'} = 0.30\,\mu\mathrm{rad}$, and $\sigma_l = 0.051\,\mathrm{m}$. The physical space occupied by the bent crystal is: $x > 1\,\mathrm{mm}$ and $|y| < 1.5\,\mathrm{mm}$. Since the dispersion $\eta$ at the position of the crystal is $-4\,\mathrm{m}$, the inner edge of the crystal in the longitudinal phase space, i.e., the $\delta$-$l$ phase space, is at $\delta \simeq 1\,\mathrm{mm}/4\,\mathrm{m} = 0.25 \times 10^{-3}$. The bucket half-height is $\delta_h = 0.26 \times 10^{-3}$ for a peak rf voltage of 20 MV.

With uncorrelated phase noise, the turn-to-turn energy variation equation is given by

$$\delta_{n+1} = \delta_n + \frac{eV}{E_0} \sin\left(\pi + 2\pi h \frac{l_n}{C_0} + \phi_n\right),$$

where $\phi_n$ is the phase noise at the $n$th traversal of the rf cavity, randomly generated according to a Gaussian distribution. It was assumed that $\phi_n$ doesn't change as the bunch of protons being followed passes through the rf. To obtain filtered phase noise, we first generate a sequence of random phase noises $\{\phi_1, \phi_2, \ldots, \phi_N\}$, and then compute the discrete Fourier transform by

$$\Phi_m = \sum_{n=1}^{N} \phi_n \exp\big(-2\pi i(m-1)(n-1)/N\big),$$

where $m = 1, 2, \ldots, N$. Since the noises are real, $\Phi_1$, $\Phi_{\frac{N}{2}+1}$ are real and $\Phi_{m'} = \Phi_m^*$ if $m' = N + 2 - m$. Thus

$$\phi_n = \frac{1}{N}\left\{\Phi_1 + \Phi_{\frac{N}{2}+1}(-1)^{n-1} + 2 \times \sum_{m=2}^{\frac{N}{2}} \mathrm{Re}\Big(\Phi_m \exp\big(2\pi i(m-1)(n-1)/N\big)\Big)\right\}.$$

Here $N$ is assumed to be even. With $n$ being the turn number, the synchrotron tune for $\Phi_m \exp\big(2\pi i(m-1)(n-1)/N\big)$ can be defined as

$$Q_m = \frac{m-1}{N}.$$

Since we want to minimize the diffusion of particles from the beam core, and the small-oscillation synchrotron tune for the SSC is

$$Q_{so} = \frac{f_s}{f_0} = \frac{4.23}{3440.93} = 0.00123,$$

we filter out the terms with $Q_m > 0.00123\alpha$ where $0 < \alpha < 1$ is the filtering fraction. Here, $f_s$ is the small-oscillation synchrotron frequency and $f_0$ the machine frequency. The resulting filtered noise, $\hat{\phi}_n$, is then given by

$$\hat{\phi}_n = \frac{2}{N}\sqrt{\frac{N}{2(m_0-1)}} \sum_{m=2}^{m_0} \mathrm{Re}\Big(\Phi_m \exp\big(2\pi i(m-1)(n-1)/N\big)\Big),$$

where $m_0 \geq 2$ is the largest integer such that $m_0 \leq 0.00123N\alpha$ and $\sqrt{\frac{N}{2(m_0-1)}}$ is a normalization factor such that both series $\phi_n$ and $\hat{\phi}_n$ have the same variance.

In our simulations using filtered noise, $\alpha = 0.85$ and $N = 10^5$ are fixed; thus, $m_0 = 104$. Figure 3 clearly shows the difference between filtered $\hat{\phi}_n$ and unfiltered $\phi_n$ with the rms value $\sigma_\phi = 0.06$. In the former case the noises are correlated over a few hundred turns whereas in the latter case the noises are completely uncorrelated from turn to turn. Shown in Figure 4 is the degree to which the beam core in the longitudinal phase space has been diluted by filtered and unfiltered noises. The initial beam profile is shown in Figure 4(a). The profile of the beam perturbed by filtered noise with $\sigma_\phi = 0.015$ after $10^6$ turns is shown in Figure 4(b); that perturbed by unfiltered noise with $\sigma_\phi = 0.06$ is shown in Figure 4(c). Clearly the beam core is diluted to a much greater degree by unfiltered noises. In $10^6$ turns the crystal receives 7 hits in the case with filtering and 8 hits in the case without filtering. Thus the extraction rate is roughly the same in both cases. Figure 5 shows the origins in the longitudinal phase space of the particles diffused to the crystal by filtered and unfiltered noises. The origins of the 65 hits obtained in $10^7$ turns using filtered noise with $\sigma_\phi = 0.015$ are shown in Figure 5(a); origins of the 160 hits obtained in $5.3 \times 10^6$ turns using unfiltered noise with $\sigma_\phi = 0.06$ are shown in Figure 5(b). Clearly the particles diffused to the crystal by filtered noise come mainly from the beam tail whereas those diffused to the crystal by unfiltered noise come rather uniformly from the whole beam. The beam profiles in the longitudinal phase space after the first hits are shown in Figure 6. Because filtered noises are correlated over a certain time interval, the beam wobbles, as evidenced in Figure 6(a) for which $\sigma_\phi = 0.06$ and the first hits occur rather early, in turn 2131. Unfiltered noise does not cause the beam to wobble, as shown in Figure 6(b) for which $\sigma_\phi = 0.06$ and the first hits occur in turn 13,006. However, when filtered noise is used with lower power, the degree to which the beam wobbles diminishes, as seen in Figure 6(c) for which $\sigma_\phi = 0.015$ and the first hits occur in turn 20,412.

A series of runs was made using filtered noise with $\sigma_\phi = 0.007$, 0.015, 0.040, 0.060, 0.069, 0.085, 0.098, and 0.155. Particles were followed for $10^6$ turns in all but two runs. In the runs with $\sigma_\phi = 0.007$ and $\sigma_\phi = 0.015$, we followed particles for $10^7$ turns in order to obtain a reasonable number of hits. Shown in Figure 7 is a log-log plot of the extraction rate $\Re$, normalized to one proton per bunch, versus $\sigma_\phi$. The plot is clearly a straight line. Thus $\Re(\sigma_\phi)$ can be parameterized as

$$\Re = a_1 \sigma_\phi^{b_1},$$

where $a_1 = 0.524$ and $b_1 = 2.403$, as determined from a $\chi^2$ fit. For $\sigma_\phi = 0.0042$, the above parameterization yields $\Re = 10^{-6}\,\mathrm{sec}^{-1}$. Assuming $10^{14}$ protons-per-beam, this gives the desired extraction rate of $10^8$ protons per second for SFT beauty physics experiments.

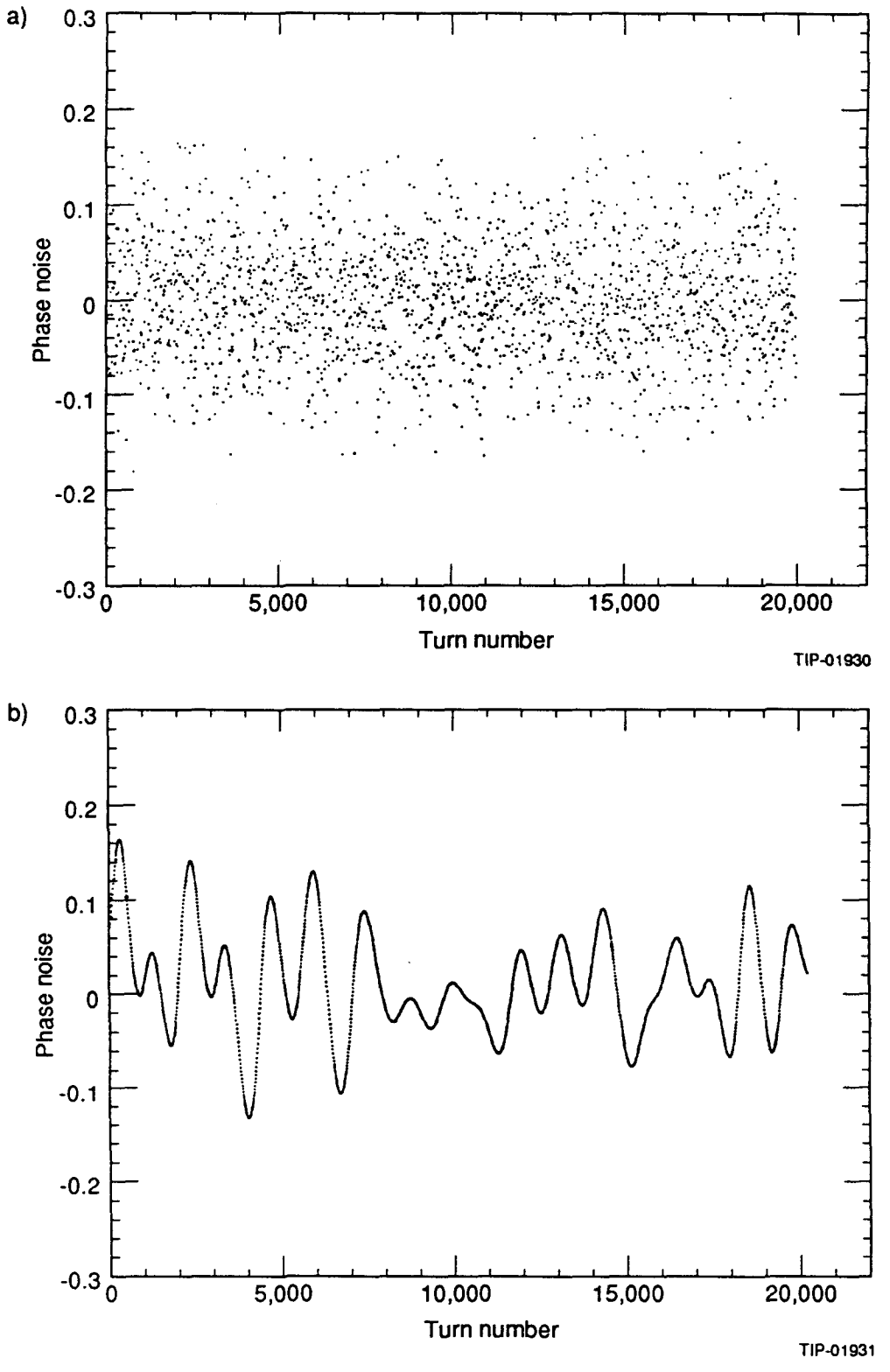


Figure 3. Phase Noises Used in the First 20,000 Turns. (a) White or unfiltered noise. (b) Filtered noise. Both cases have a standard deviation of 0.06. The filtering fraction is 0.85.

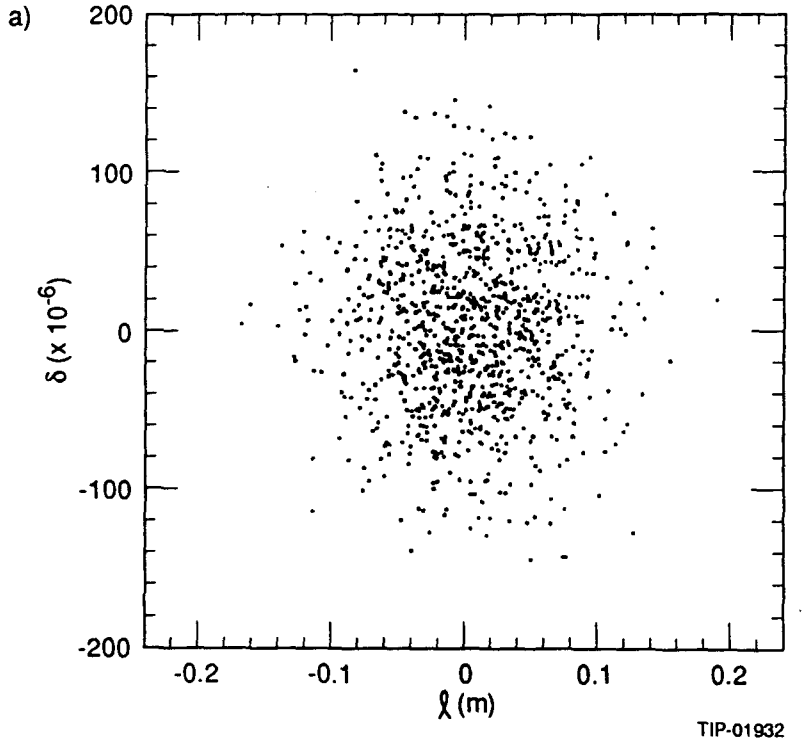


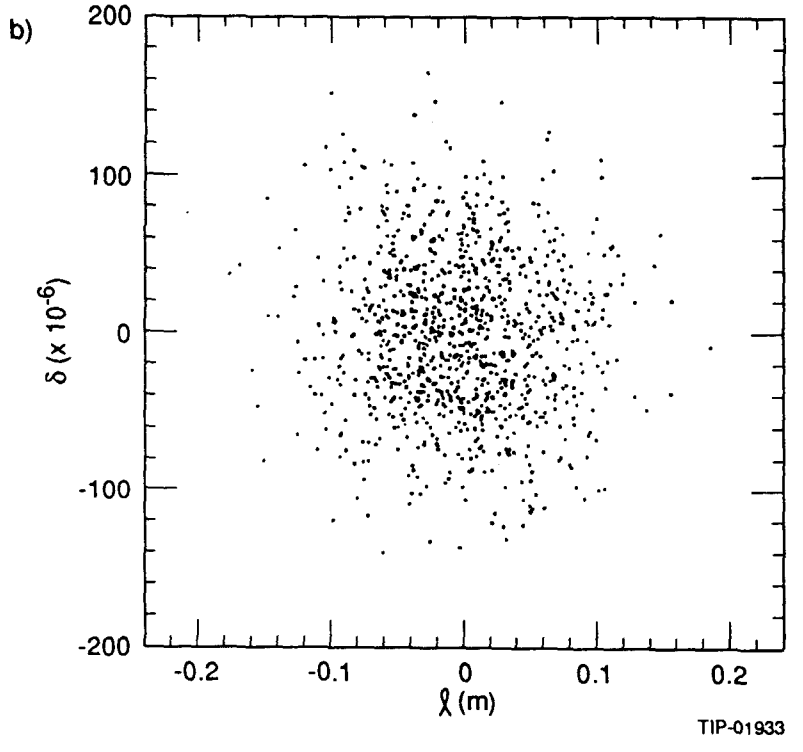


Figure 4. Beam Profiles in Longitudinal Phase Space. (a) The initial beam profile. (b) The final profile of the beam perturbed by filtered noise with a standard deviation of 0.015 after $10^6$ turns.

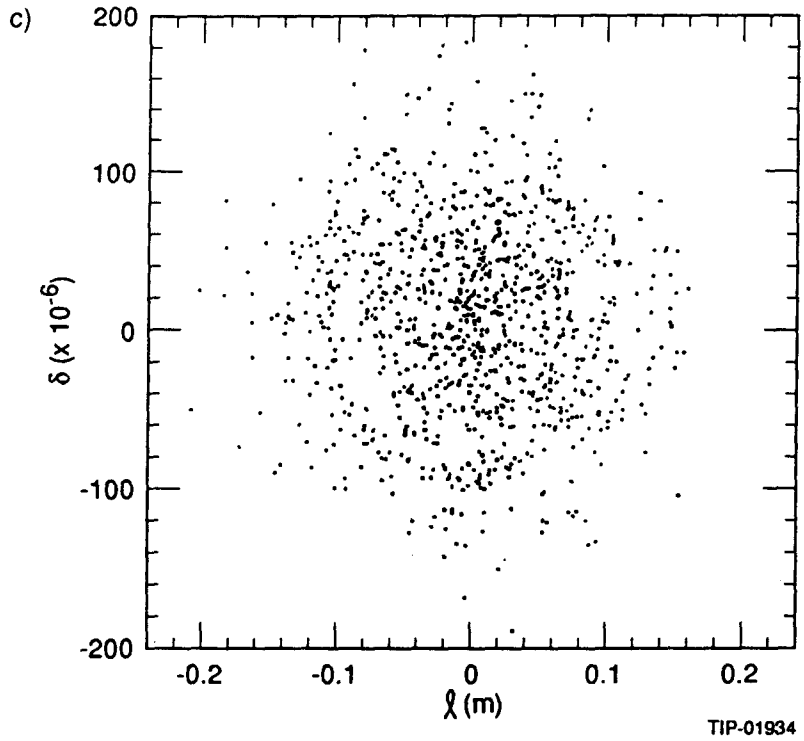


Figure 4. (Cont.) (c) The final profile of the beam perturbed by unfiltered noise with a standard deviation of 0.06 after $10^6$ turns.

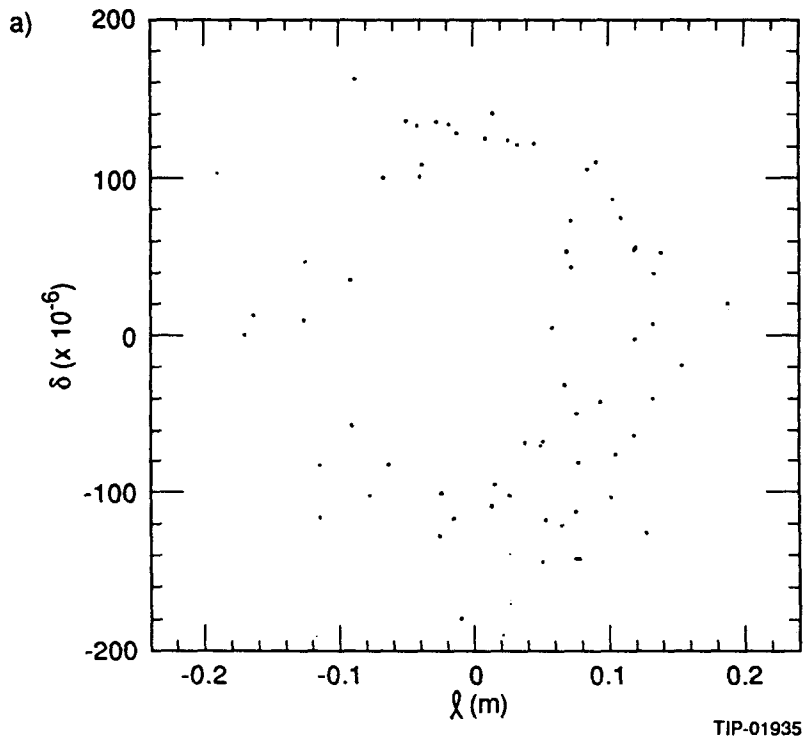


Figure 5. Origins of the Hits in Longitudinal Phase Space. (a) Origins of the hits obtained in $10^7$ turns using filtered noise with a standard deviation of 0.015.

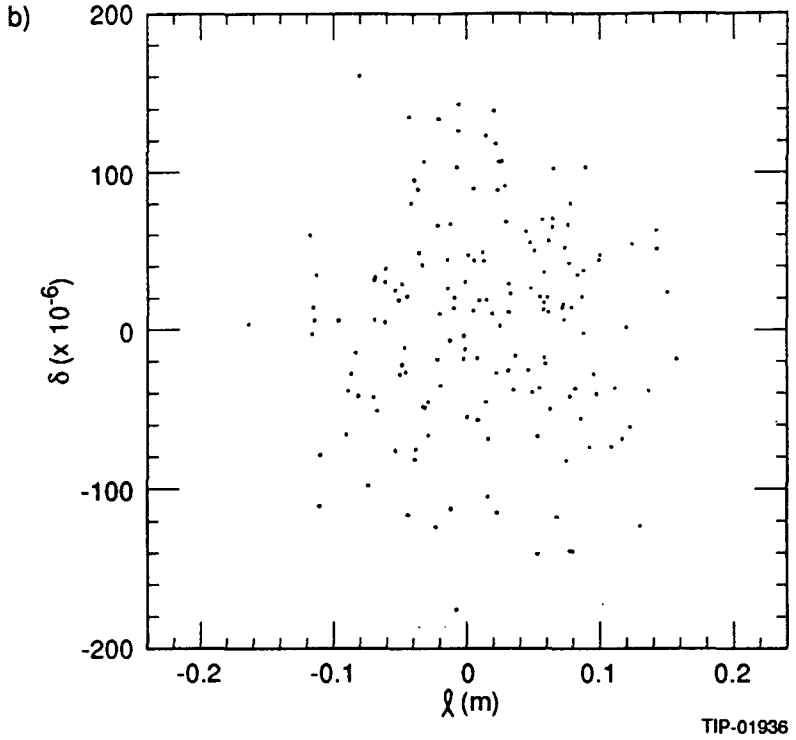


Figure 5. (Cont.) (b) Origins of the hits obtained in $5.3 \times 10^6$ turns using unfiltered noise with a standard deviation of 0.06.

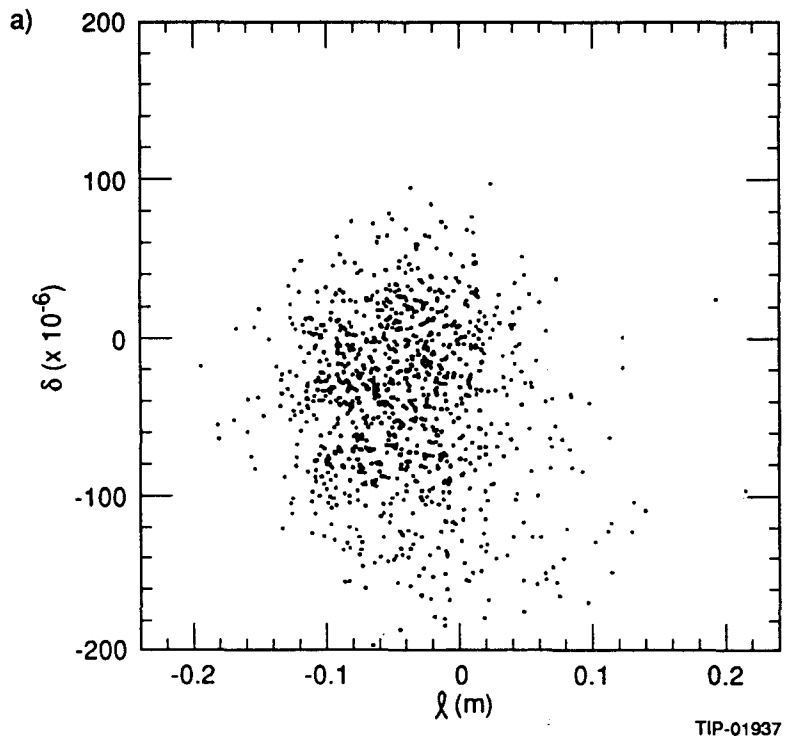


Figure 6. Beam Profiles in Longitudinal Phase Space After the First Hits. (a) The profile of the beam perturbed by filtered noise with a standard deviation of 0.06. The first hits occur in turn 2131.

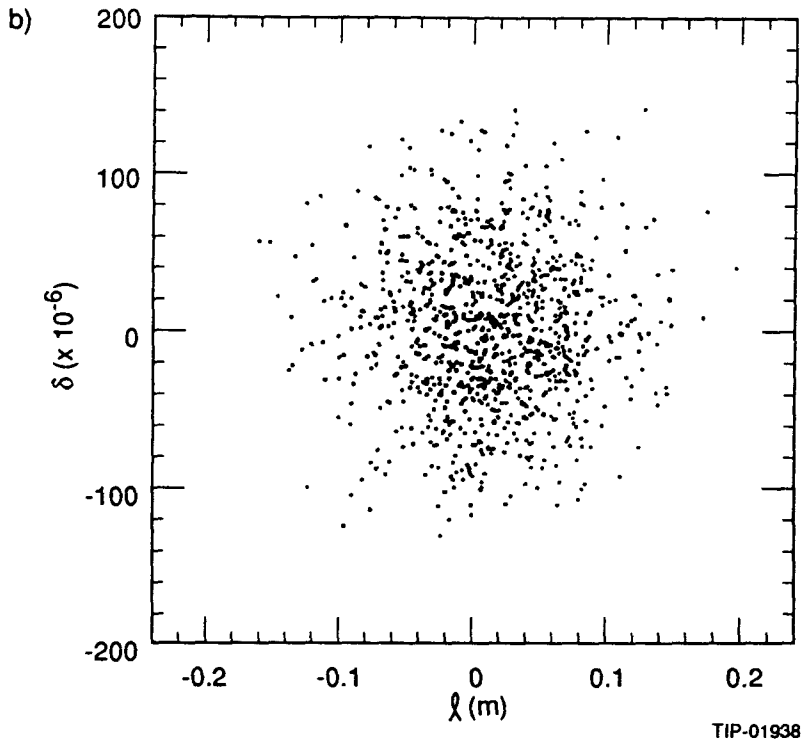


Figure 6. (Cont.) (b) The profile of the beam perturbed by unfiltered noise with a standard deviation of 0.06. The first hits occur in turn 13,006.

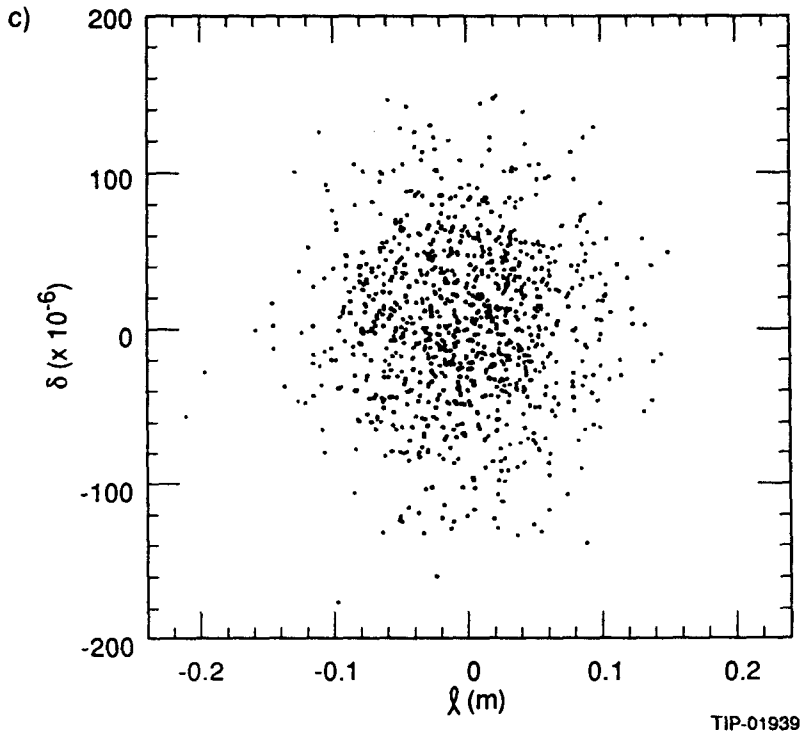


Figure 6. (Cont.) (c) The profile of the beam perturbed by filtered noise with a standard deviation of 0.015. The first hits occur in turn 20,412.

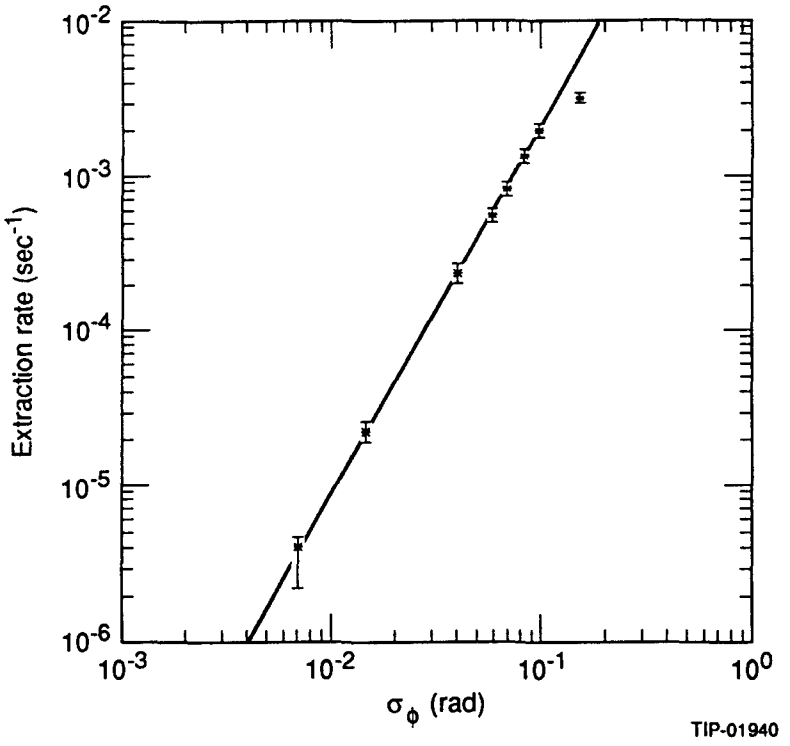


Figure 7. Extraction Rate $\Re$ Normalized to One Proton-Per-Bunch as a Function of the Noise Standard Deviation $\sigma_\phi$. The points with error bars are the simulation results. The straight line is the fit: $\Re = a_1 \sigma_\phi^{b_1}$ with $a_1 = 0.524$ and $b_1 = 2.403$.

The width of the distribution of the hits in the horizontal coordinate $x$, i.e., the standard deviation in $x$ from the inner edge of the bent crystal $x = 1\,\text{mm}$, was found to decrease as the noise standard deviation decreases. This is shown in Figure 8. The distribution width for noise standard deviations smaller than 0.007 should be as thin as, if not thinner than, that for the noise standard deviation of 0.007, which is $\sim 2\,\text{microns}$. In order to accommodate such a thin distribution in $x$ of the hits, the effective septum width, which is determined by the polishing of the crystal edge, should be minimized.

## 3.0 DEFLECTION EFFICIENCY OF THE SSC BEAM BY A BENT SILICON CRYSTAL

In this section our analytical estimates and computer simulations on single passage deflection efficiency of the SSC beam are presented. For more details concerning the theory and numerical simulation involved, readers are directed to Reference 14. A Si crystal bent along (110) planes with constant curvature is assumed throughout.

### 3.1 Analytical Estimates

A relativistic charged particle with energy $E$ will be captured into the channeling regime by a planar channel of a bent crystal when

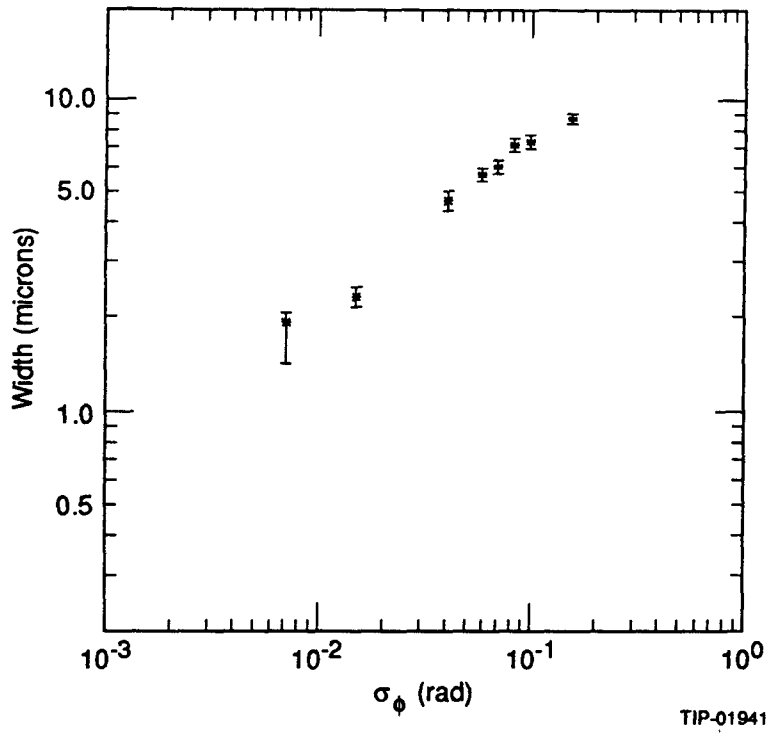


Figure 8. Width of the Distribution of the Hits in the Horizontal Coordinate $x$ as a Function of the Noise Standard Deviation $\sigma_\phi$. The width is defined to be the root-mean-square (rms) deviation in $x$ from the inner edge of the bent crystal $x = 1\,\mathrm{mm}$.

$$E_{y0} = U_{\mathrm{eff}}(y_0, R) + \frac{E}{2}\theta_{y0}^2 < E_{yc}(R),$$

where $y_0, \theta_{y0}, E_{y0}$ are the initial transverse coordinate, angle, and energy of the incident particle, respectively; $U_{\mathrm{eff}}(y, R)$ is the effective potential of a bent channel;[13] $E_{yc}$ is the critical transverse energy for channeling; and $R$ is the bend radius of the crystal. Here the transverse coordinate $y$ is measured from the plane. The trajectory of a channeled particle is stable when it does not approach closer to a channel wall than the critical distance $y_c$. For high-energy particles the critical distance is $y_c \simeq u_1$, where $u_1$ is the rms amplitude of the thermal vibrations of the crystal atoms (0.075 Å for Si). Thus, the critical transverse energy in a bent crystal for existence of stable particle trajectories in a planar channel is

$$E_{yc}(R) = U_{\mathrm{eff}}(y_c, R).$$

The efficiency of the surface capture $P_c$ of particles into stable channeling states may be determined as

$$P_c(R) = 2\int_{y_c}^{y_h} p(y_0)dy_0 \int_0^{\theta_{m0}} p(\theta_{y0})d\theta_{y0},$$

$$\theta_{m0} = \theta_{m0}(y_0, R) = \sqrt{\frac{2}{E}\left(E_{yc}(R) - U_{\text{eff}}(y_0, R)\right)},$$

where $p(y_0)$, $p(\theta_{y0})$ are the initial spatial and angular distributions of incident particles, and $y_h$ is the other root of the equation $U_{\text{eff}}(y, R) = E_{yc}(R)$. When the angular distribution of the beam is Gaussian with the rms angle $\overline{\theta_y}$, and the spatial distribution of the beam is uniform, we have

$$P_c(R, \overline{\theta_y}) = \frac{1}{d_p} \int_{y_c}^{y_h} \text{erf}\left(\sqrt{\frac{E_{yc}(R) - U_{\text{eff}}(y_0, R)}{E\overline{\theta_y}^2}}\right) dy_0,$$

where $d_p$ is the channel width.

The channeled fraction of the beam will decrease due to multiple scattering by crystal electrons and nuclei according to

$$N_{ch}(s; R, \overline{\theta_y}) \propto \exp\left(-\frac{s}{S_{1/e}(R, \overline{\theta_y})}\right),$$

where $s$ is the path length measured from the entrance and $S_{1/e}$ is the dechanneling length of the beam. The dechanneling half-length $S_{1/2}$ of particles may be estimated as[14]

$$S_{1/2}(R, \overline{\theta_y}) = \frac{E_{yc}(R)}{A(R, \overline{\theta_y})}.$$

The friction coefficient $A$ in the transverse energy space is averaged over the trajectories and the ensemble of channeled particles,

$$A(R, \overline{\theta_y}) = \left\langle \frac{\overline{\delta E_y}}{\delta s} \right\rangle = \frac{E}{2} \int_0^{E_{yc}} p(E_{y0}) dE_{y0} \int_{y_1}^{y_2} \frac{\overline{(\delta\theta_y)^2}}{\delta s}(y) \frac{dy}{v_y(y, E_{y0})} \Bigg/ \int_{y_1}^{y_2} \frac{dy}{v_y(y, E_{y0})},$$

where $p(E_{y0})$ is the initial transverse energy distribution of the beam, $v_y$ is the transverse particle velocity, $\overline{(\delta\theta_y)^2}/\delta s$ is the mean square of the deflection angle projection per unit length due to multiple scattering by crystal electrons and nuclei, and $y_1$, $y_2$ are the coordinates of the particle turning points in the effective potential.

The volume capture of protons into the channeling states,[14] can be neglected when the bend radius $R$ is less than $\sim 10\,R_c$, where $R_c$ is the critical bend radius. Then the efficiency of deflecting a beam with a given angular divergence $\overline{\theta_y}$ by an angle $\theta_B$ through a bent crystal of bend radius $R$ may be determined as

$$P_d(\theta_B; R, \overline{\theta_y}) = P_c(R, \overline{\theta_y}) \exp\left(-\frac{\theta_B R}{S_{1/e}(R, \overline{\theta_y})}\right).$$

The critical bend radius $R_c = E/eE_{max}$, where $E_{max}$ is the maximal strength of the averaged field of atomic planes. For a Si crystal bent along (110) planes, $eE_{max} = 6\,\mathrm{GeV/cm}$ and $R_c = 33.3\,\mathrm{m}$ for $20\,\mathrm{TeV}$ protons.

Figures 9–11 show the surface capture probability $P_c$, the dechanneling length $S_{1/e}$, and the deflection efficiency $P_d$ as a function of bend radius $R$ for a Si crystal bent along (110) planes, a $20\,\mathrm{TeV}$ proton beam with the angular divergence $\overline{\theta_y} = 0.30\,\mu\mathrm{rad}$, and a deflection angle $\theta_B = 100\,\mu\mathrm{rad}$. The planar potential and electron density in the crystal were calculated in the Moliere approximation with the thermal vibrations of crystal atoms included, i.e., a thermally averaged Moliere potential.

The calculations were made with two different values of $y_c$: $u_1$ and $2.5\,u_1$. Increasing $y_c$, the captive efficiency $P_c$ decreases (Figure 9). For the dechanneling length $S_{1/e}$, the reverse picture is observed (Figure 10). At $y_c = u_1$, the dechanneling length increases before it decreases, as the bend radius decreases. This is because, in a slightly bent crystal, a part of the large amplitude trajectories is in a region of smaller electron and nuclei densities than in a straight crystal, as shown in Figure 12.

When $R$ becomes less than $\sim 10\,R_c$, both $P_c$ and $S_{1/e}$ decrease rapidly. As the bend radius increases, the deflection efficiency reaches a maximum at some bend radius $R_m$ (Figure 11) and then decreases because the crystal length increases with increasing bend radius for a fixed deflection angle thereby increasing particle dechanneling. Thus, the optimal conditions for beam deflection, i.e., the bend radius $R_m$ and the corresponding crystal length $S_m = \theta_B R_m$, can be selected. In both cases ($y_c = u_1$ and $2.5\,u_1$), $R_m \approx 1500\,\mathrm{m}$ and $S_m \approx 15\,\mathrm{cm}$, and the corresponding deflection efficiencies are $P_d(y_c = u_1) = 0.8588$ and $P_d(y_c = 2.5u_1) = 0.7468$.

### 3.2 Computer Simulations

Our analytical estimates of deflection efficiency are dependent on the selection of the critical distance $y_c$. Here computer simulations are used to investigate this dependence for the case of single passage of the SSC beam through a bent crystal.

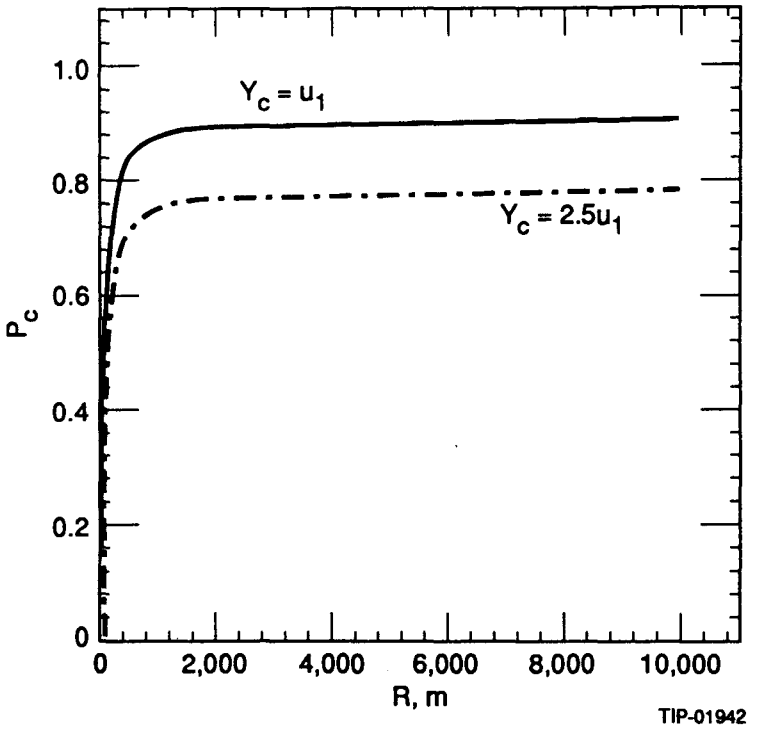


Figure 9. Capture Efficiency $P_c$ of the SSC Beam into the Channeling Regime as a Function of the Crystal Bend Radius $R$. $y_c$ is the critical approach of a particle to a channel wall. The beam vertical divergence is $\overline{\theta_y} = 0.30\mu$rad.

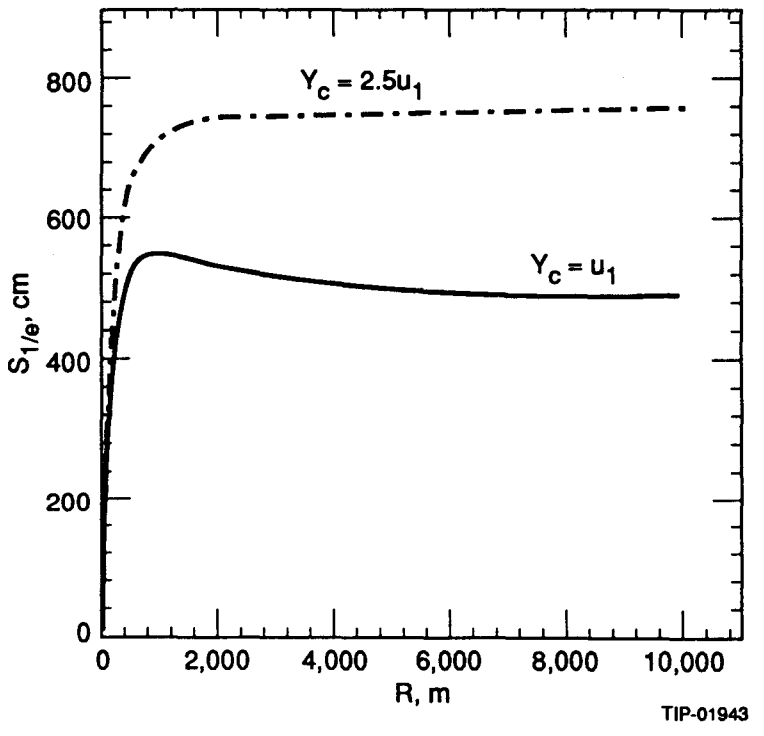


Figure 10. The Dechanneling Length $S_{1/e}$ of the SSC Beam as a Function of the Crystal Bend Radius $R$.

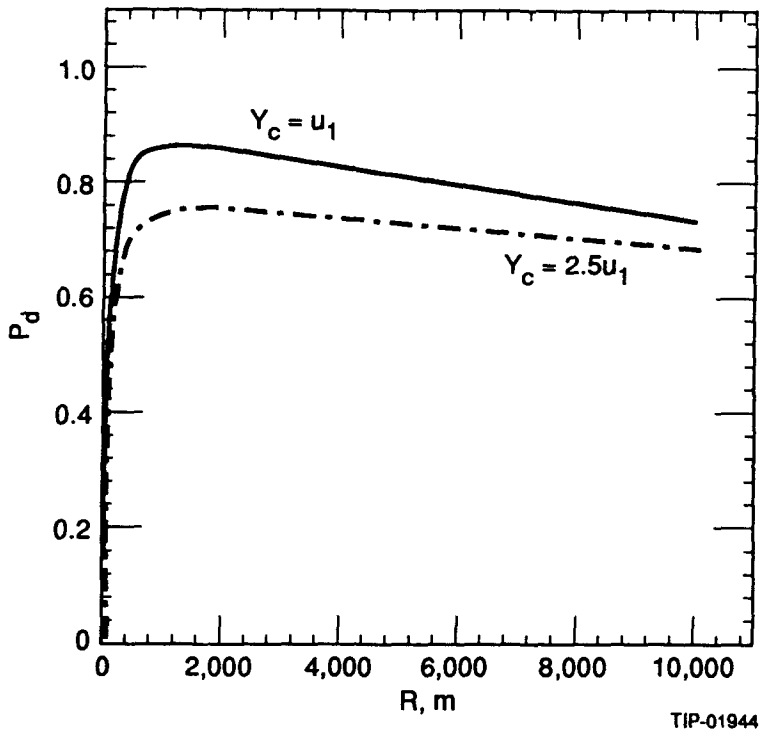


Figure 11. The Deflection Efficiency $P_d$ of the SSC Beam as a Function of the Crystal Bend Radius $R$ for a Deflection Angle $\alpha = 100\mu$rad.

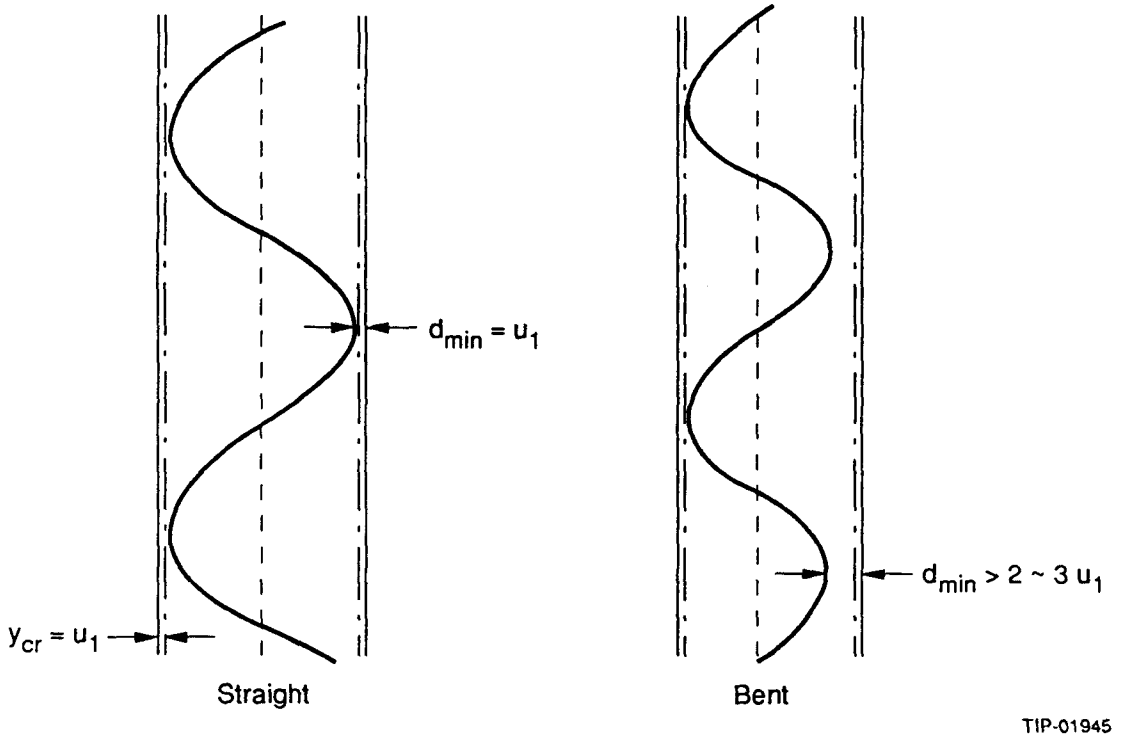


Figure 12. Illustration of Particle Trajectories with Large Amplitude Oscillations in a Straight and a Slightly Bent Crystal.

In the first-order approximation, ignoring multiple scattering, the particle trajectories in a bent crystal were calculated by numerically solving the equations of motions in the effective potential of bent atomic planes:[14]

$$\ddot{y}(t) = -\frac{c^2}{E}\frac{d}{dy}U_{\text{eff}}(y, R),$$
$$\dot{s}(t) = (v_0^2 - \dot{y}^2(t))^{1/2},$$

where $v_0$ is the particle velocity and $y$, $s(\dot{y}, \dot{s})$ are the transverse and longitudinal coordinates (velocities) respectively. When the particle has passed through a crystal layer $\Delta s = 10\,\mu\text{m} \ll \lambda$, where $\lambda$ is the wavelength of particle oscillations in the channel, the change in the transverse velocity due to multiple scattering is computed as $\Delta v_y = v_0 \Delta\theta_y$. The projection of deflection angle, $\Delta\theta_y$, was chosen from a zero-mean Gaussian distribution with variance

$$\langle\overline{(\Delta\theta_y)^2}\rangle = v_0 \int_{y_{\text{in}}}^{y_{\text{out}}} \frac{\overline{(\delta\theta_y)^2}}{\delta s}(y)\,\frac{dy}{v_y(y, E_y)},$$

where $y_{\text{in}}$, $y_{\text{out}}$ are the entry and exit coordinates respectively of the particle passing through the considered layer $\Delta s$.

Shown in Figure 13 are the simulation results on deflection efficiencies $P_d$ of the SSC beam by a bent Si crystal for different bend radii $R$, as well as analytical estimates using two different values of $y_c$: $u_1$ and $2.5\,u_1$. The simulation results are closer to the analytical estimates with $y_c = u_1$. This is because with the considered crystal lengths $S < S_m \ll S_{1/e}$, the channeled particles with large oscillation amplitudes in bent channels are not lost and thus contribute to the deflection efficiency. According to our simulations, the maximum deflection efficiency of the SSC beam by a bent Si crystal may be about 80%.

## 4.0 MULTI-TURN EXTRACTION EFFICIENCY

Due to the injection of filtered noise in the rf cavity, particles near the beam edge in the longitudinal phase space begin to hit the crystal. In the simulations on multi-turn extraction of the SSC beam, a phase noise of a large standard deviation $\sigma_\phi = 0.5$ filtered at $\alpha = 0.85$ has been used so that particles are quickly diffused to the crystal, thereby greatly reducing computing time. Of the particles that strike the crystal, some will fail to be channeled and some will be channeled initially but become dechanneled after traveling a certain length in the crystal because of electron and nuclear multiple scattering. Some of the particles that fail to be channeled all the way through the crystal will be lost due to nuclear inelastic interactions, and the remaining will be scattered out of the crystal. If a

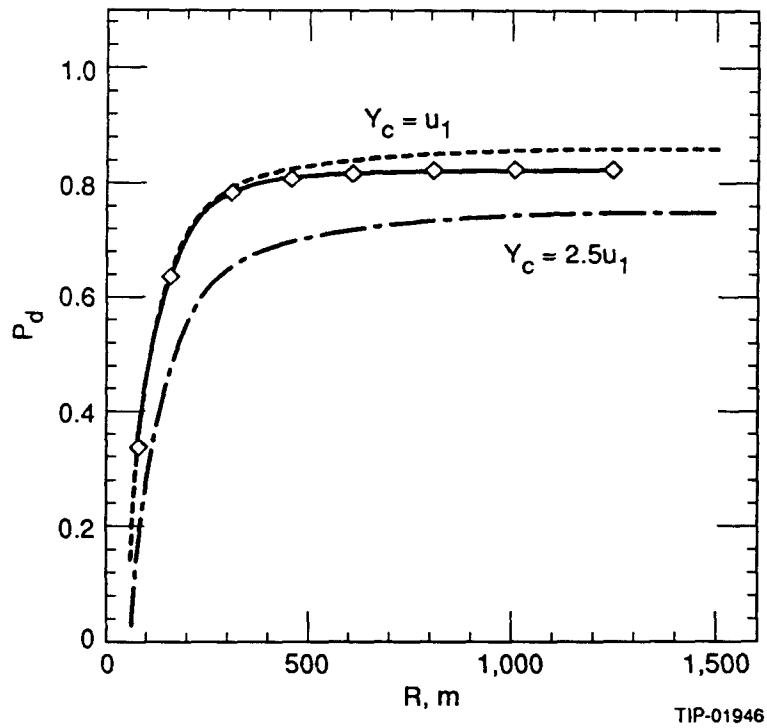


Figure 13. Simulation Results on the Deflection Efficiency of the SSC Beam (Diamonds) in Comparison with the Analytic Estimates (Curves).

particle is channeled all the way through the crystal and exits with an angle $y' > \theta_B - \theta_c$, it is assumed to be extracted from the accelerator. If a particle exits from the crystal with an angle $\theta_1 < y' < \theta_B - \theta_c$, it is assumed to be lost downstream at the wall of the beam tube. Here the acceptance angle $\theta_1$ at the position of the crystal is determined by

$$\theta_1 = \frac{r_2}{\sqrt{\beta_{y,1}\,\beta_{y,2}}},$$

where $r_2$ is the radius of the beam tube, $\beta_{y,1}$ is the vertical beta function at the position of the crystal, and $\beta_{y,2}$ is the maximal vertical beta function in the SSC lattice downstream of the crystal. Assuming $\beta_{y,1} = 500\,\mathrm{m}$, $\beta_{y,2} = 300\,\mathrm{m}$ (a typical value in a regular cell), and $r_2 = 1\,\mathrm{cm}$ for the radius of the beam tube, the acceptance angle $\theta_1$ is $\sim 25\,\mu\mathrm{rad}$. Only the particles that exit with an angle $y' < \theta_1$ are to remain in the beam and have the probability to be channeled on subsequent passes.

The extraction efficiency can increase substantially due to multiple passage of particles through the crystal, when the beam broadening by multiple scattering in the crystal is not too large, i.e.,

$$\theta_{ms} \lesssim \theta_c \quad \text{or} \quad S \lesssim S_{ms}.$$

and when the beam loss due to inelastic nuclear interactions is small, i.e.,

$$S \ll S_n.$$

Here $\theta_{ms}$ is the rms angle of multiple scattering through the crystal, $S_{ms}$ is the length of the crystal through which the rms angle of multiple scattering is equal to the channeling critical angle $\theta_c$, and $S_n$ is the inelastic nuclear interaction length of the crystal. For Si, $S_{ms} = 42\,\text{cm}$ and $S_n = 45.5\,\text{cm}$.

For a Si crystal bent along (110) planes by a fixed angle of $100\,\mu$rad, Figure 14 shows the dependence upon the bend radius $R$ of (1) the fraction of the particles extracted from multiple passage ($P_{ex}$), (2) the fraction of the particles extracted from single passage ($P_{ex}^1$), (3) the fraction of the particles lost in the crystal due to inelastic nuclear interactions ($P_{nuc}$), and (4) the total fraction of the particles lost either in the crystal or at the pipe wall ($P_{los}$). $P_{los}$ is minimal at $R \sim 300\,\text{m}$. For $R > 300\,\text{m}$, the dominant cause of particle loss is the multiple scattering of channeled particles by crystal electrons and nuclei; thus the particle loss decreases with decreasing $R$. For $R < 300\,\text{m}$, the dominant cause of particle loss is the failure of being captured into the channeling regime upon the entrance into the crystal; thus the particle loss increases with decreasing $R$. The dependence of $P_{ex}$ on $R$ has the reverse character. It is maximal at $R \sim 300\,\text{m}$, where it equals about 93%. This is more than the maximal deflection efficiency $P_d$ (Figure 13). The increase from $P_{ex}^1$ to $P_{ex}$ increases with decreasing $R$ and can be more than 50% for crystals of large curvature.

Figure 15 shows the distribution of extracted particles in the number of passages through the crystal for a bend radius of $R = 150\,\text{m}$. The majority of extracted particles have a passage multiplicity less than 5. Figure 16 and Figure 17 show the distribution of extracted particles in the horizontal coordinate $x$ at the entrance into the crystal for bend radii of $R = 150\,\text{m}$ and $R = 1500\,\text{m}$, respectively. The inside edge of the crystal is at $x = 1\,\text{mm}$. The distribution width is about $10 \sim 15\,\mu$m. In Figure 16 (for the $R = 150\,\text{m}$ case) the distribution of the extracted particles with passage multiplicity greater than 1 is shown separately by a solid line. These particles give a long tail up to $400 \sim 500\,\mu$m.

## 5.0 CONCLUSIONS

Computer simulations have been used to investigate the method of injecting filtered phase noise into the rf system to create a large amplitude beam halo for bent crystal extraction. It has been shown that the protons diffused to the bent crystal came from the tails, not the core of the beam, and that unlike the "white" noise which is turn-to-turn

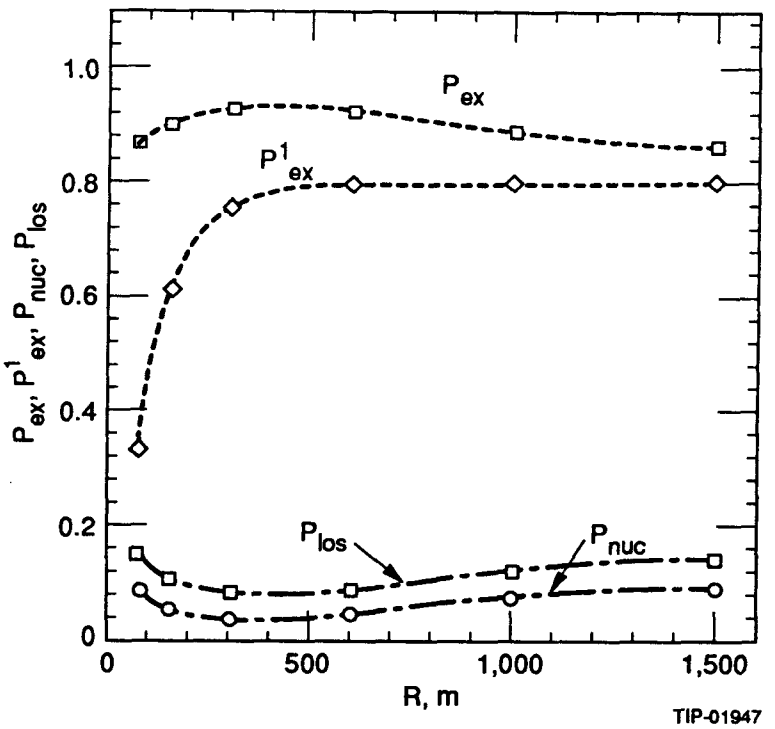


Figure 14. Dependence on the Crystal Bend Radius $R$ of the Multi-Turn Extraction Efficiency $P_{ex}$ of the SSC Beam, as well as Those of the Extraction Efficiency $P^1_{ex}$ from the First Passage Through the Crystal, the Fraction $P_{nuc}$ of the Particles Lost in the Crystal and the Total Fraction $P_{los}$ of the Particles Lost Either in the Crystal or at the Wall of the Beam Tube.

uncorrelated, the filtered noise was correlated over many machine revolutions and thus caused the beam to wobble. However, the degree to which the beam wobbles was shown to diminish as the noise standard deviation decreases. The rate at which the protons are diffused to the bent crystal by phase noise filtered at a fraction of 0.85 was found to depend linearly on the noise standard deviation raised to a power of 2.4, from which a noise standard deviation of 0.0042 was extrapolated for the extraction rate desired in SFT physics experiments. The distribution width in the horizontal coordinate of the hits was shown to decrease with decreasing standard deviation of filtered noise and to approach a value no greater than $\sim 2$ microns as the noise standard deviation approaches 0.0042.

Both theory and simulation have been used to investigate the channeling efficiencies of an incident beam by a bent silicon crystal. It has been shown that the critical distance of closest approach inside which a channeled particle will become dechanneled is well approximated by the rms amplitude of thermal vibrations of the crystal lattice. For a bent silicon crystal with a constant bend angle, it has been shown that the channeling efficiency due to single (multiple) passage, as the bend radius increases, increases rapidly for bend radii smaller than 300 (200) m, remains essentially constant for bend radii between

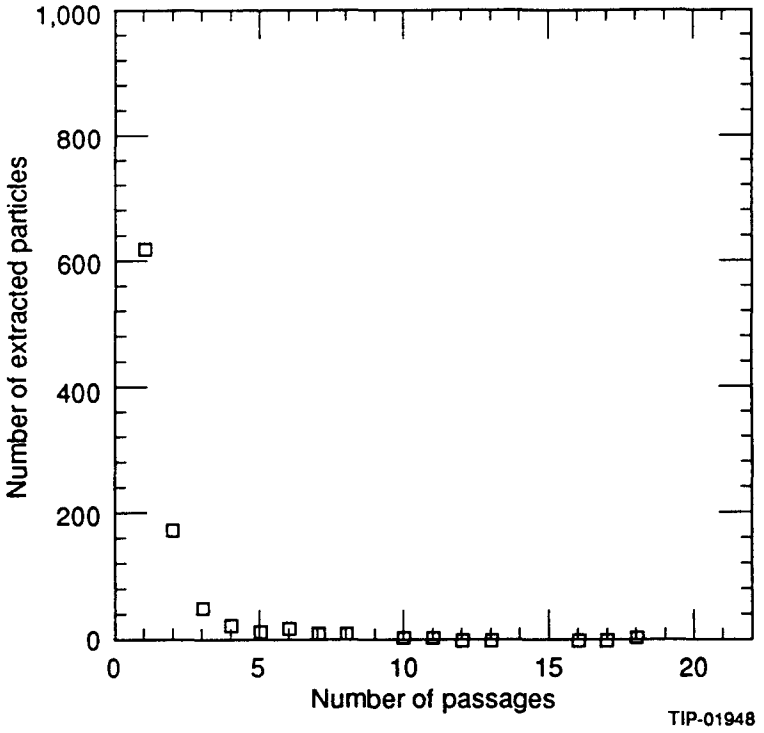


Figure 15. Distribution of the Particles Extracted from the SSC in the Number of Passages Through a Si Crystal of Bend Radius $R = 150\,\mathrm{m}$.

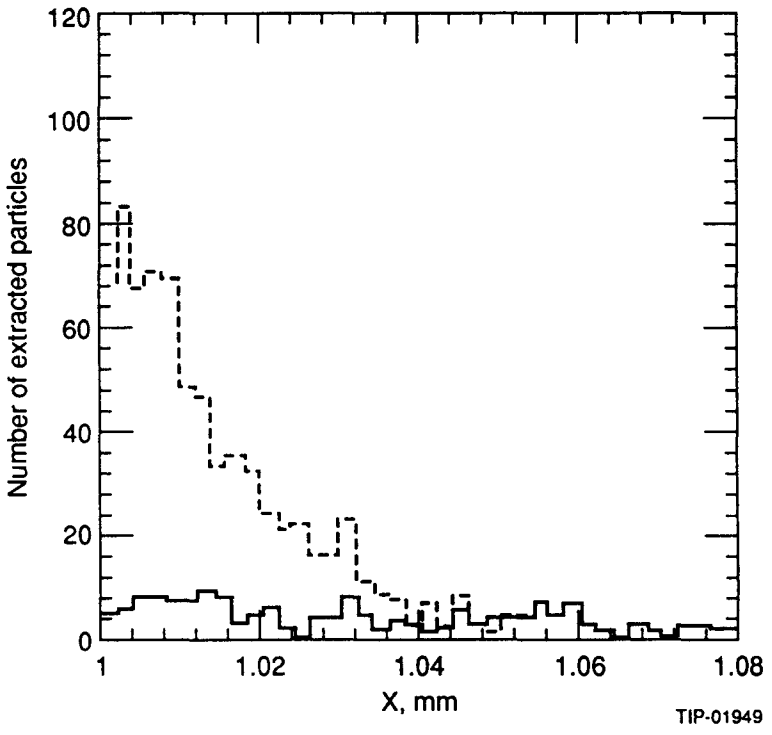


Figure 16. Distribution of the Particles Extracted from the SSC in the Horizontal Coordinate $x$ at the Entrance into a Si Crystal of Bend Radius $R = 150\,\mathrm{m}$. The dashed line represents the total distribution and the solid line represents the distribution of the extracted particles with passage multiplicity greater than 1.

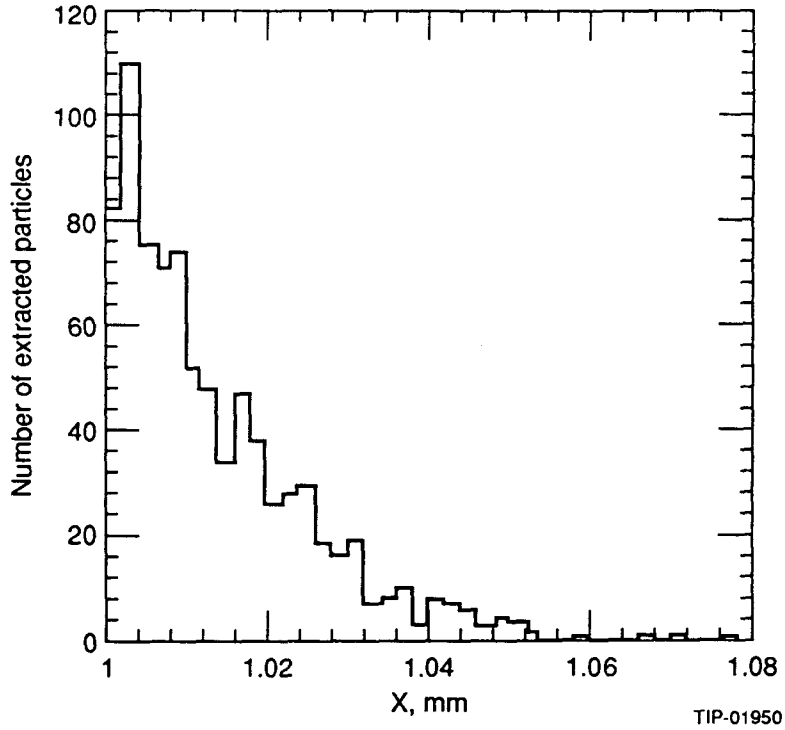


Figure 17. Distribution of the Particles Extracted from the SSC in the Horizontal Coordinate $x$ at the Entrance into a Si Crystal of Bend Radius $R = 1500$ m (Only the Total Distribution is Shown).

300 (200) m and 1500 (500) m, and decreases slowly for bend radii greater than 1500 (500) m. The maximal channeling efficiency due to single (multiple) passage was shown to be $\sim 80\%$ ($\sim 93\%$).

## ACKNOWLEDGEMENTS

The authors would like to thank D. Carrigan, Jr., and A. Chao, B. Cox, J. Ellison, T. Murphy, B. Newberger, S. Peggs, and E. Tsyganov for suggestions and discussions. In particular, Alex Chao's support for this work, Jim Ellison's review of the manuscript, and Al Garren's effort in modifying the SSC lattice are gratefully acknowledged.

## REFERENCES


1. B. Cox et al., "The Possibility of Parasitic 20 TeV Beams Extracted from the SSC Using Bent Crystals," *Proc. 1988 Summer Study on the Design and Utilization of the SSC*, Snowmass (1988) p. 536.

2. The SFT Collaboration, *An Expression of Interest in a Super Fixed Target Beauty Facility at the SSC*, EOI-14, submitted to the SSC PAC, 25 May 1990.

3. C.H. Sun et al., "Slow Parasitic Extraction at the SSC Using Crystal Septa," *Proc. 1984 Summer Study on the Design and Utilization of the SSC*, Snowmass (1984) p. 483.

4. R.A. Carrigan, Jr., T.E. Toohig, and E.N. Tsyganov, *Beam Extraction from TeV Accelerators Using Channeling in Bent Crystals*, Nucl. Instr. and Meth. **B48** (1990) 167.

5. B. Newberger et al., *Summary Report of Working Sessions on Bent Crystal Beam Extraction for the SSC*, SSC Laboratory Report SSCL-N-722, June 1990.

6. B. Newberger and H.J. Shih, *Low Intensity Beam Extraction at the SSC*, SSC Laboratory Report SSCL-344, January 1991.

7. E.N. Tsyganov, *Some Aspects of the Mechanism of a Charged Particle Penetration through a Monocrystal*, Fermilab TM-682, Batavia (1976).

8. E.N. Tsyganov, *Estimates of Cooling and Bending Processes for Charged Particle Penetration through a Monocrystal*, Fermilab TM-684, Batavia (1976).

9. S.I. Baker et al., *Deflection of Charged Particles in the Hundred GeV Regime Using Channeling in Bent Single Crystals*, Phys. Lett. **137B** (1984) 129.

10. D.S. Gemmell, *Channeling and Related Effects in the Motion of Charged Particles through Crystals*, Rev. Mod. Phys. **46** (1974) 129.

11. J.F. Bak et al., *Detailed Investigation of Channeling Phenomena Involved in Bending of High-Energy Beams by Means of Crystals*, Nucl. Phys. **B242** (1984) 1.

12. Al Garren, personal communication.

13. A.M. Taratin et al., *Theory of Planar Channeling of Relativistic Protons in Bent Crystals*, Phys. Stat. Sol. **B 100** (1980) 273.

14. A.M. Taratin and S.A. Vorobiev, *Planar Dechanneling and Volume Capture of High-Energy Protons in a Bent Crystal*, Nucl. Instr. and Meth. **B47** (1990) 247.